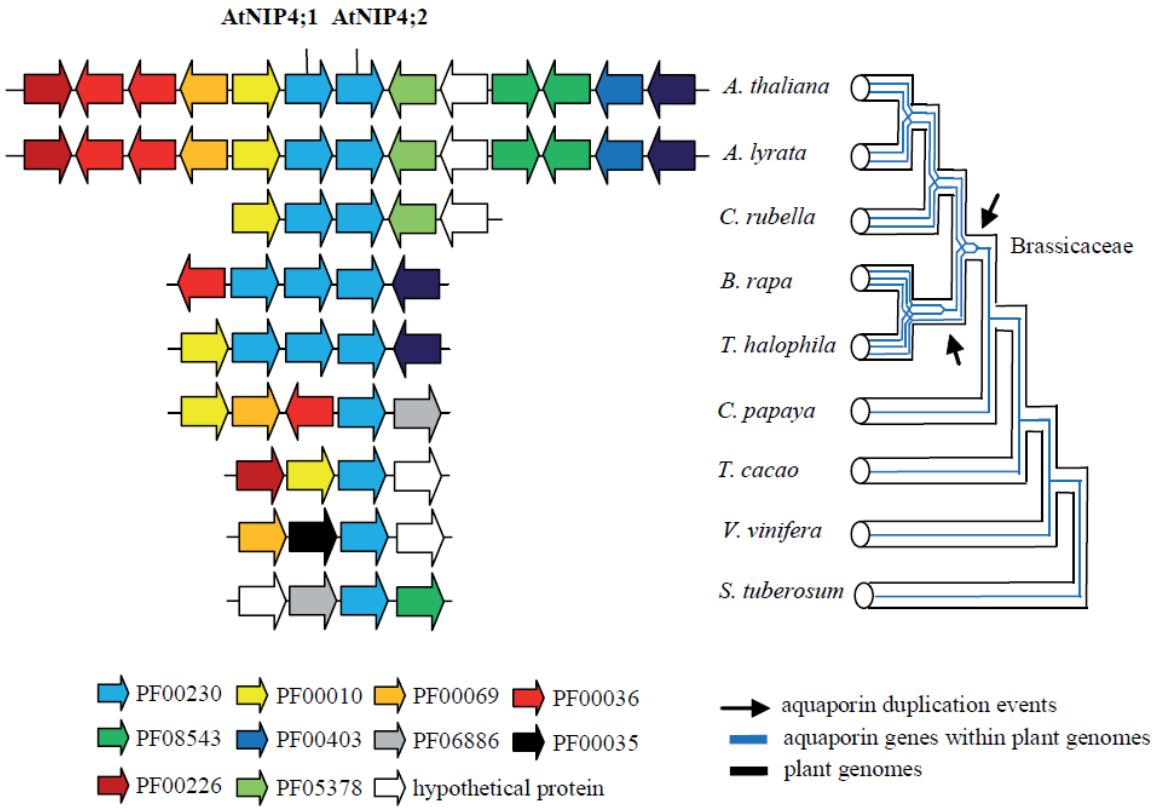

Supplemental Figure 1. Synteny analysis of *NIP4;1* and *NIP4;2*.
Examination of the *NIP4;1-NIP4;2* region in *Arabidopsis thaliana* and equivalent evolutionary regions in other dicot genomes are shown on the left panel. Phylogenetic relationships among plants and *A. thaliana NIP4;1-NIP4;2* deduced from syntenic analysis are indicated in the right panel. Genomes (putative AQP loci): *Arabidopsis thaliana* (AT5G37810, AT5G37820), *Arabidopsis lyrata* (Loc330314, Loc891407), *Capsella rubella* (Carubv10006501m, Carubv10007677m), *Brassica rapa* (rapaBra025437, rapaBra025436, rapaBra02543), *Thellungiella halophila* (Thhalv10028080m, Thhalv10027876m, Thhalv10028303m), *Carica papaya* (evm.model.supercontig_65.137), *Theobroma cacao* (Thecc1EG019213t1), *Vitis vinifera* (GSVIVT01030857001) and *Solanum tuberosum* (PGSC0003DMP400053063). PF00230: AQP protein, PF00010: helix-loop-helix DNA-binding domain containing protein, PF00069: protein kinase family protein, PF00036: OsCam2 - Calmodulin, PF08543: kinase, pfkB family, PF00403: heavy-metal-associated domain-containing protein, PF06886: Targeting protein for Xklp2, PF00035: Double-stranded RNA binding motif, F00226: dnaJ domain containing protein, PF05378 5-oxoprolinase.

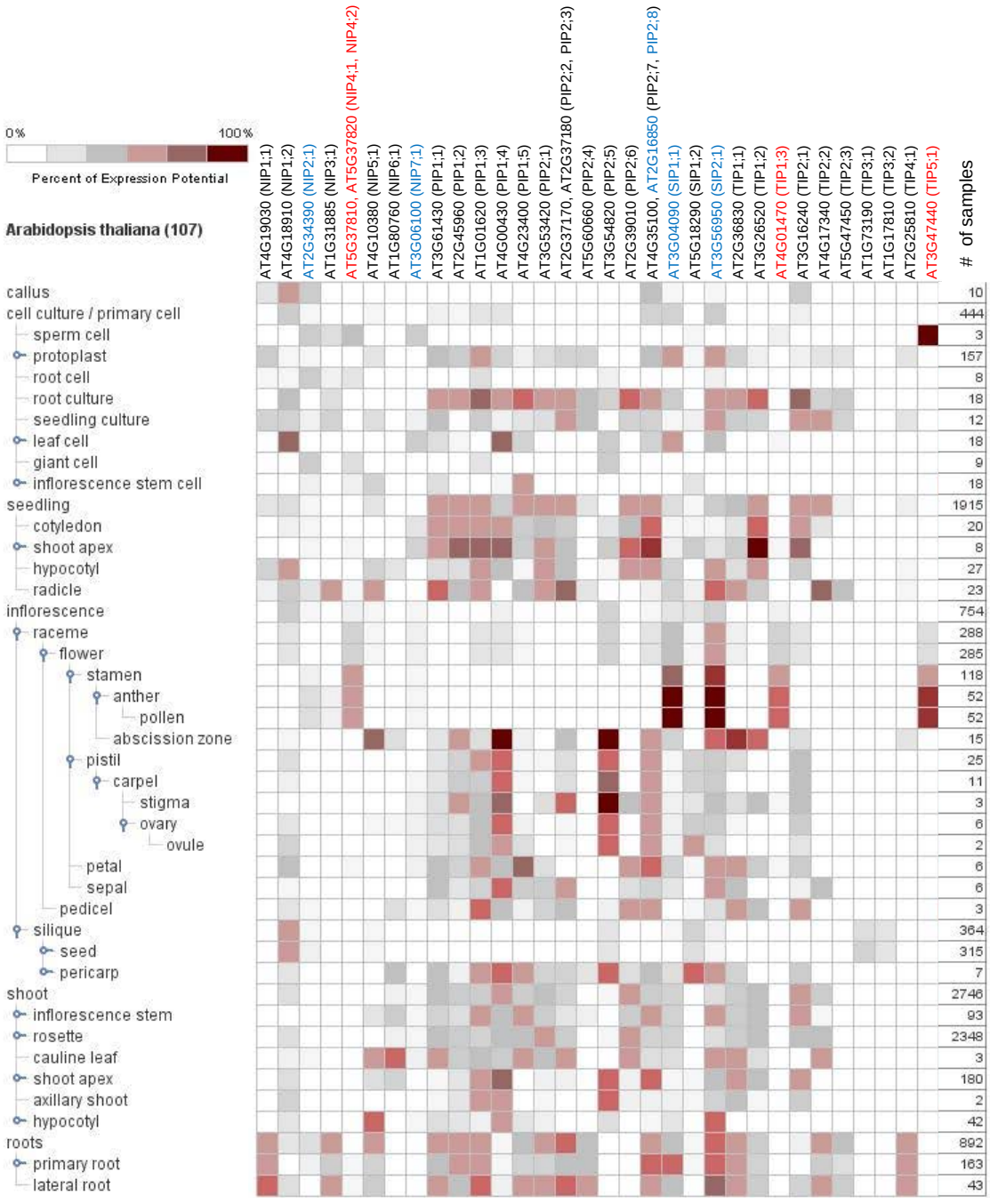

Supplemental Figure 2. Expression patterns of *Arabidopsis thaliana* aquaporin genes.
Heat map of normalized absolute expression values of 35 *Arabidopsis thaliana* AQP genes obtained using GENEVESTIGATOR (www.genevestigator.com/gv/). Pollen-specific AQPs are in red and AQPs expressed in pollen and also in sporophytic tissues are in blue (107 microarrays consulted).

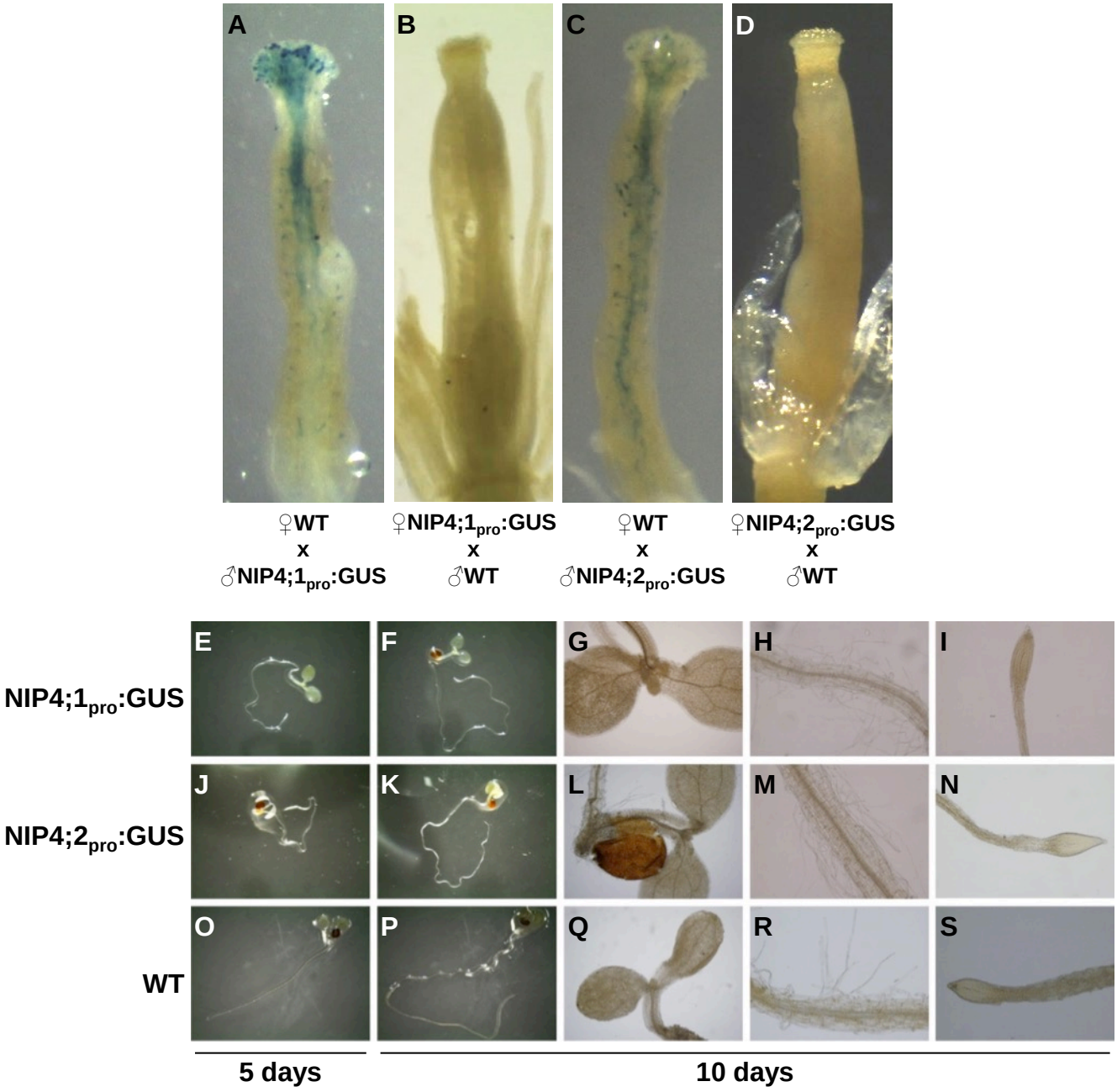

Supplemental Figure 3. GUS staining of pistils and seedlings.
GUS staining of WT pistils crossed with transgenic NIP4;1_{pro}:GUS (A) and *NIP4;2*$_{pro}$:GUS (C) pollen, and reciprocal crosses (B,D). Transgenic NIP4;1_{pro}:GUS (E-I) and NIP4;2_{pro}:GUS (J-N) seedlings grown for 5 and 10 days in 0.8% agar supplemented with Basta 12.5 mg/L. WT plants were used as control (O-S).

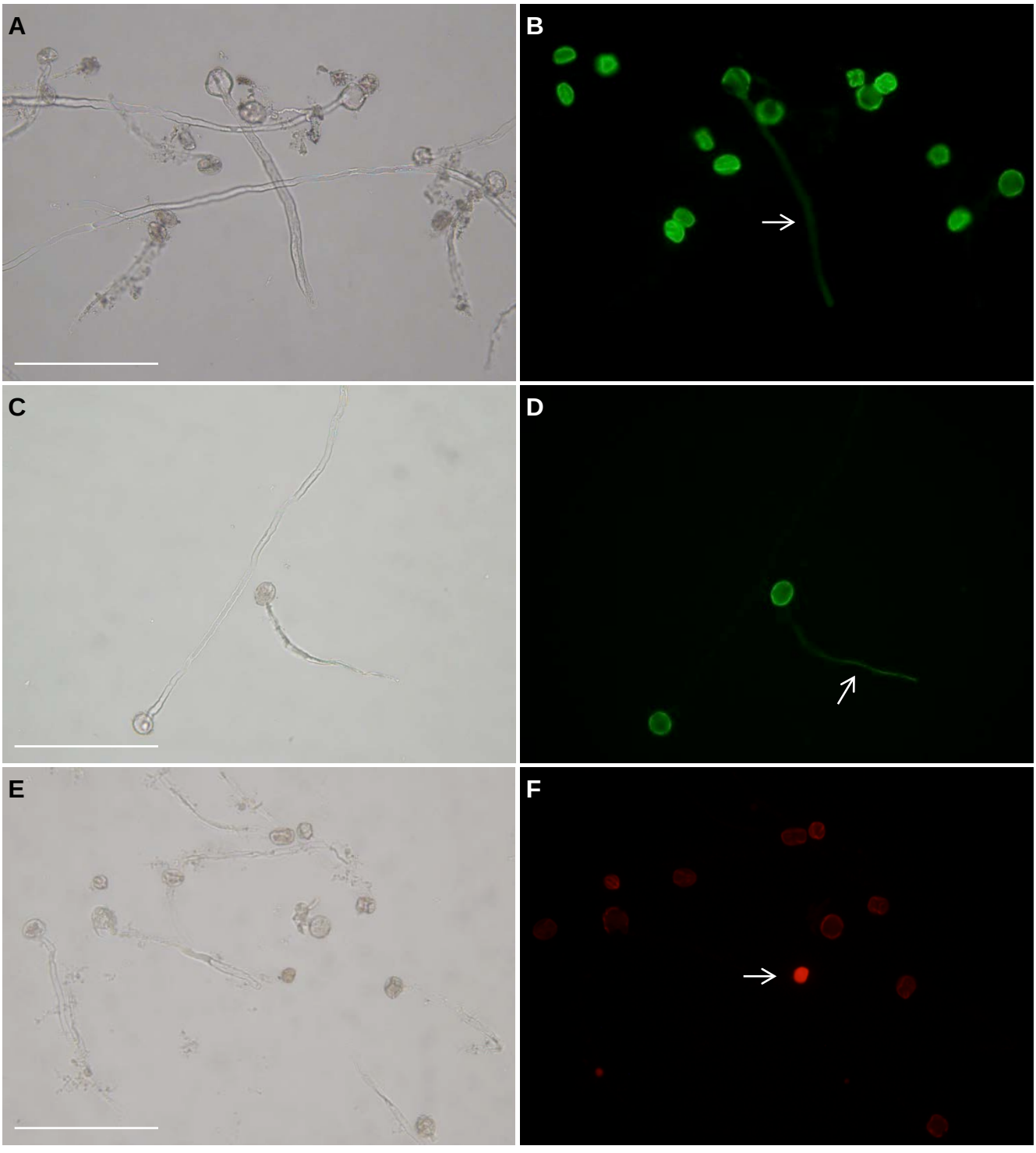

Supplemental Figure 4. Pollen bombardment assays.
Constructs *EGFP-NIP4;1* (A,B), *EGFP-NIP4;2* (C,D) and *LAT52*$_{pro}$*:RFP-LAT52*$_{pro}$*:ami356* (E,F) were validated by tobacco pollen bombardment and epifluorescence microscopy. White arrows indicate positive pollen tubes (B,D) and a pollen grain (F). Bar = 200 µm.

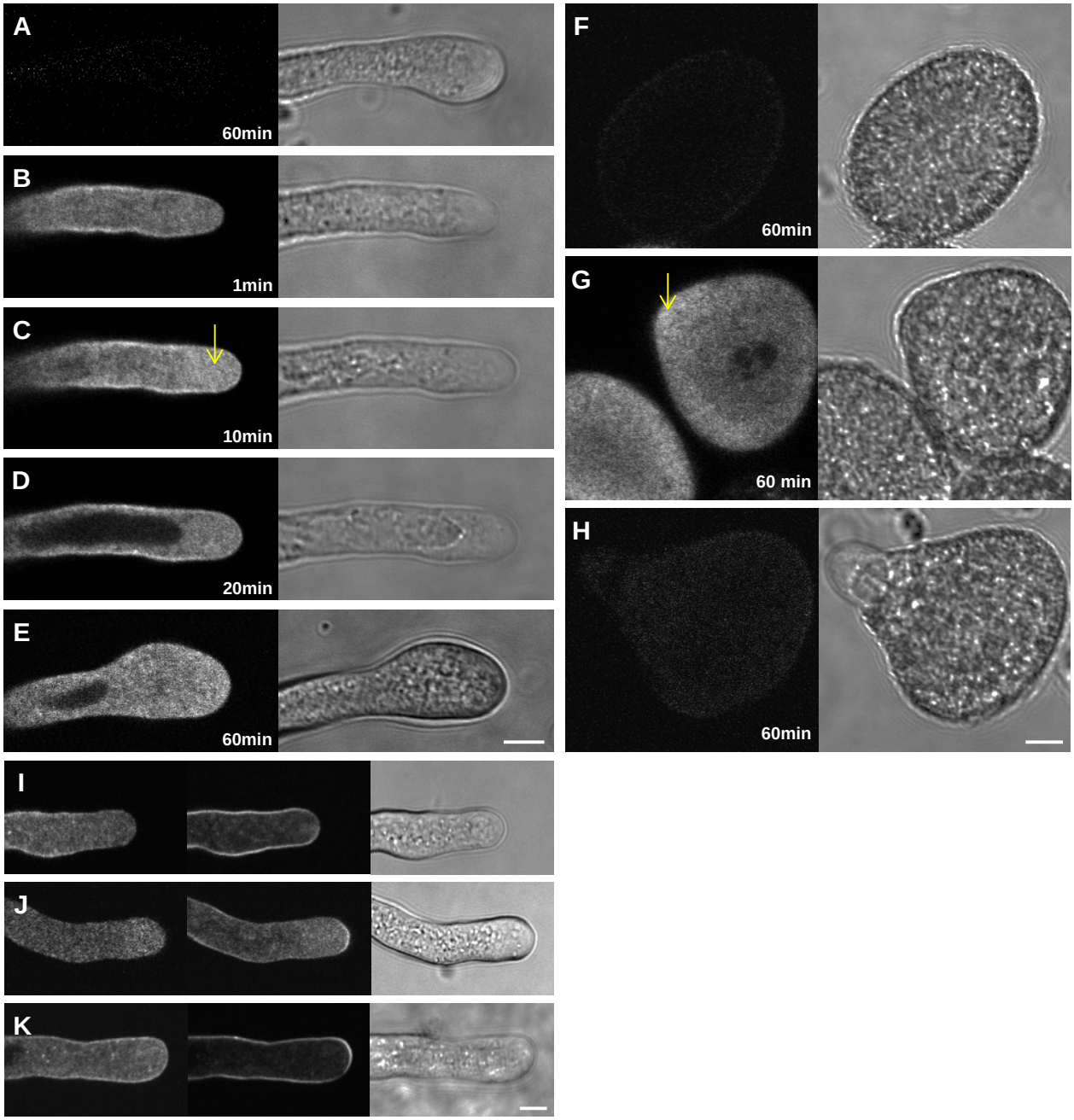

Supplemental Figure 5. Disruption of EGFP-NIP4;1 cycling.
(A-H) Arabidopsis pollen tubes were germinated for 30 min in PGM and then treated with 3 µg/ml BFA before imaging using a confocal microscope for up to 60 min. Representative fluorescence confocal images (left panels) and differential interference contrast (DIC) optics (right panels). Bar = 10 µm. (A) Effect of BFA treatment for 60 min in a WT pollen tube, showing the formation of a bubble tip as control of growth arrest. (B-E) Effect of BFA treatment on EGFP-NIP4;1 pollen tubes (line *WT/NIP4;1-20*) after 1 (B), 10 (C), 20 (D) and 60 min (E). (F) Effect of BFA treatment for 60 min in a WT grain used as control. (G) Effect of BFA treatment for 60 min on EGFP-NIP4;1 mature pollen. (H) Effect of BFA treatment for 60 min on EGFP-NIP4;2 mature pollen, used as negative control. (I-K) Arabidopsis pollen tubes were germinated for 30 min in PGM and then treated with 1 µM FM4-64 and either with 6 µg/ml BFA or 100 µM A23. Fluorescence confocal images of GFP and FM4-64 signals and DIC are shown. Bar = 10 µm. (I) GFP and FM4-64 signal in a $LAT52_{pro}$:EGFP-NIP4;1 pollen tube as control. (J) Effect of BFA treatment on a EGFP-NIP4;1 pollen tube after 25 min. (K) Effect of A23 treatment on a EGFP-NIP4;1 pollen tube after 10 min. A total of 13 independent germinations analyzing at least 20 grains and pollen tubes for each genotype and condition were performed.

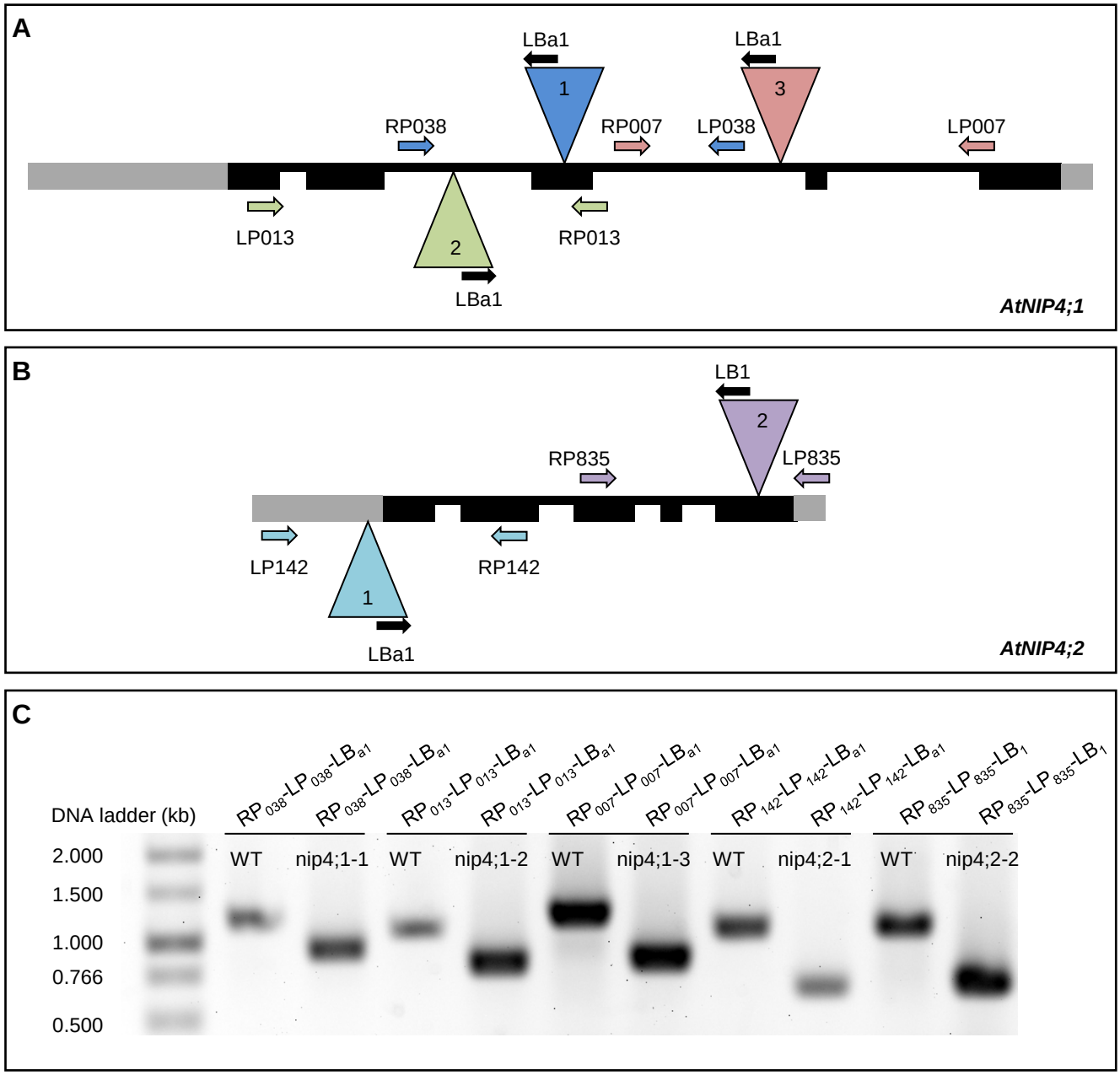

Supplemental Figure 6. Single T-DNA *nip4;1* and *nip4;2* mutant lines.
Schematic diagram of *NIP4;1* (A) and *NIP4;2* (B) genes. Black boxes represent exons, and predicted promoter and 5'and 3' UTRs are shown as grey boxes. T-DNA insertions are indicated with different colored triangles. Right (RP) and Left (LP) primers used for genotyping are indicated with arrows using the same colors as the triangles. Left border primer (LB) is also shown. (C) Genotyping PCRs were performed from genomic DNA (gDNA) from homozygous mutant plants *nip4;1-1*, *nip4;1-2*, and *nip4;1-3* and *nip4;2-1* and *nip4;2-2*, using line-specific sets of RP, LP and LB primers. WT gDNA was used as control in each PCR.

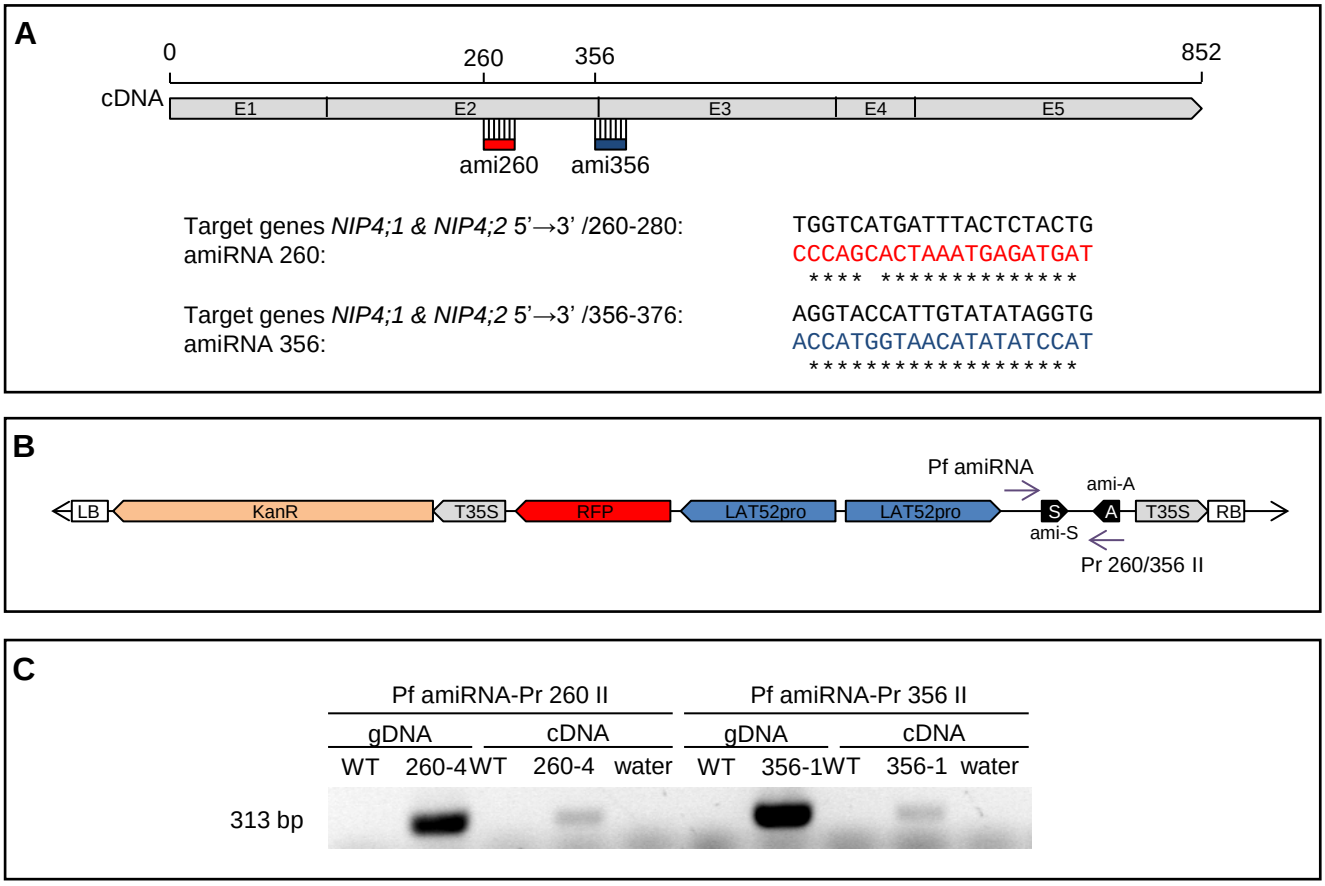

Supplemental Figure 7. Double knockdown amiRNA lines.
(A) Schematic description of the hypothesized duplexes formed by interactions between *NIP4,1* and *NIP4;2* genes and the two amiRNAs (ami260 and ami356). Paired bases are indicated by asterisks. (B) Schematic diagram of binary plasmid pK7WG2D expressing amiRNA sense (ami-S) and antisense (ami-A) sequences. The $LAT52_{pro}$:RFP reporter gene was included in the construct to identify pollen carrying the amiRNAs. Forward (Pf amiRNA) and reverse (Pr 260 II and 356 II) primers used for genotyping PCR and RT-PCR assays are indicated with arrows. (C) Genotyping PCRs with genomic DNA (gDNA) and RT-PCR assays (cDNA) from double knockdown ami260-4 and ami356-1 plants, using line-specific primers. WT gDNA and WT cDNA were used as control.

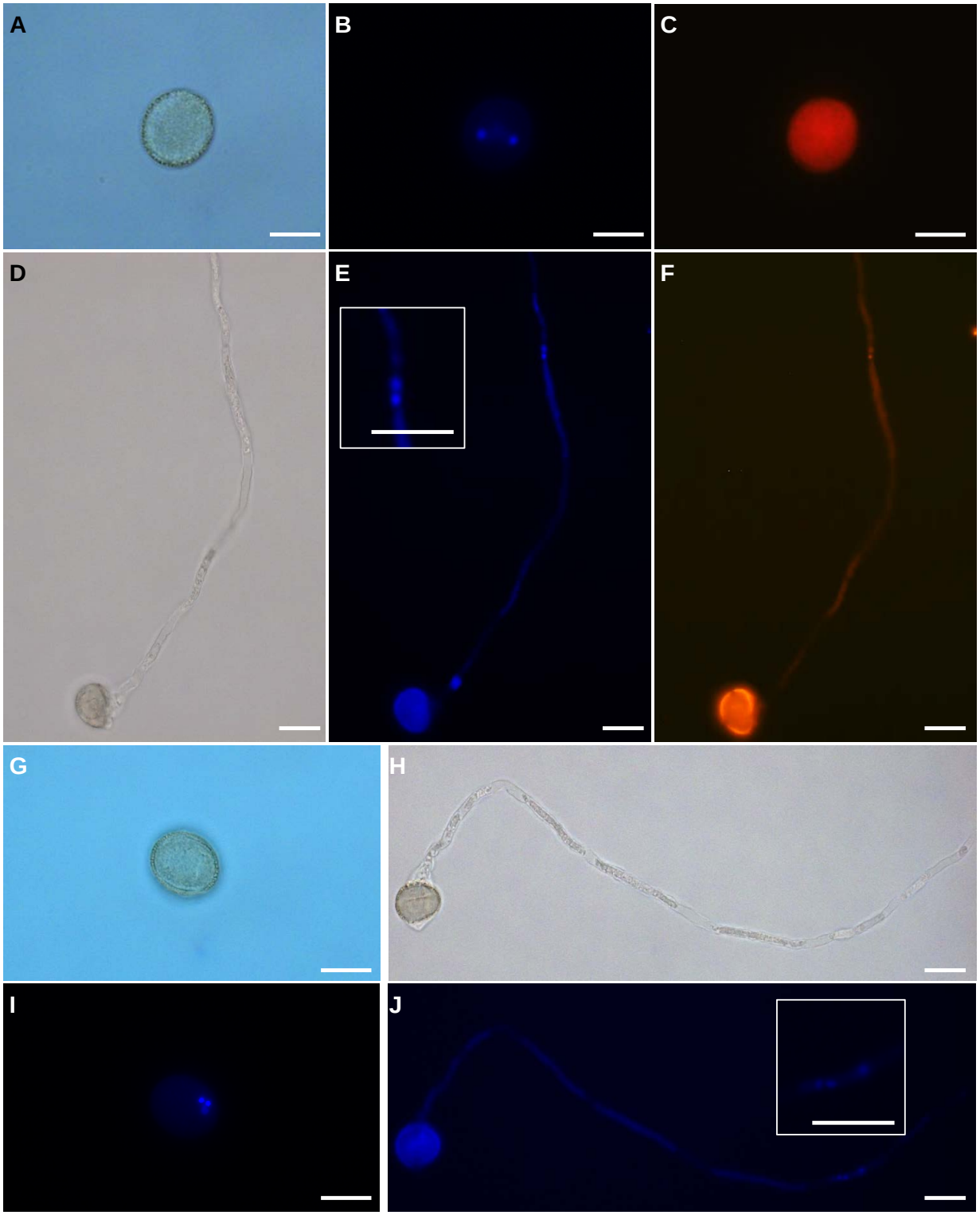

Supplemental Figure 8. Double knockdown amiRNA lines expressing the RFP reporter gene.
(A, D, G, H) Bright-field images. (B, E, I, J) Epifluorescence images showing nuclei stained with Hoechst 33342 (blue filter), and insets in E and J showing the three nuclei in detail. (C, F) Epifluorescence images showing RFP expression (red filter). (A-C) Mature pollen grain of the ami260-4 line. Bar = 20 µm. (D-F) Pollen tube of the ami356-1 line germinated in vitro for 4h. Bar = 50 µm. WT pollen grain (G, I) and tube (H, J) were included as controls. Bar = 20 µm (G,I) and 50 µm (H-J).

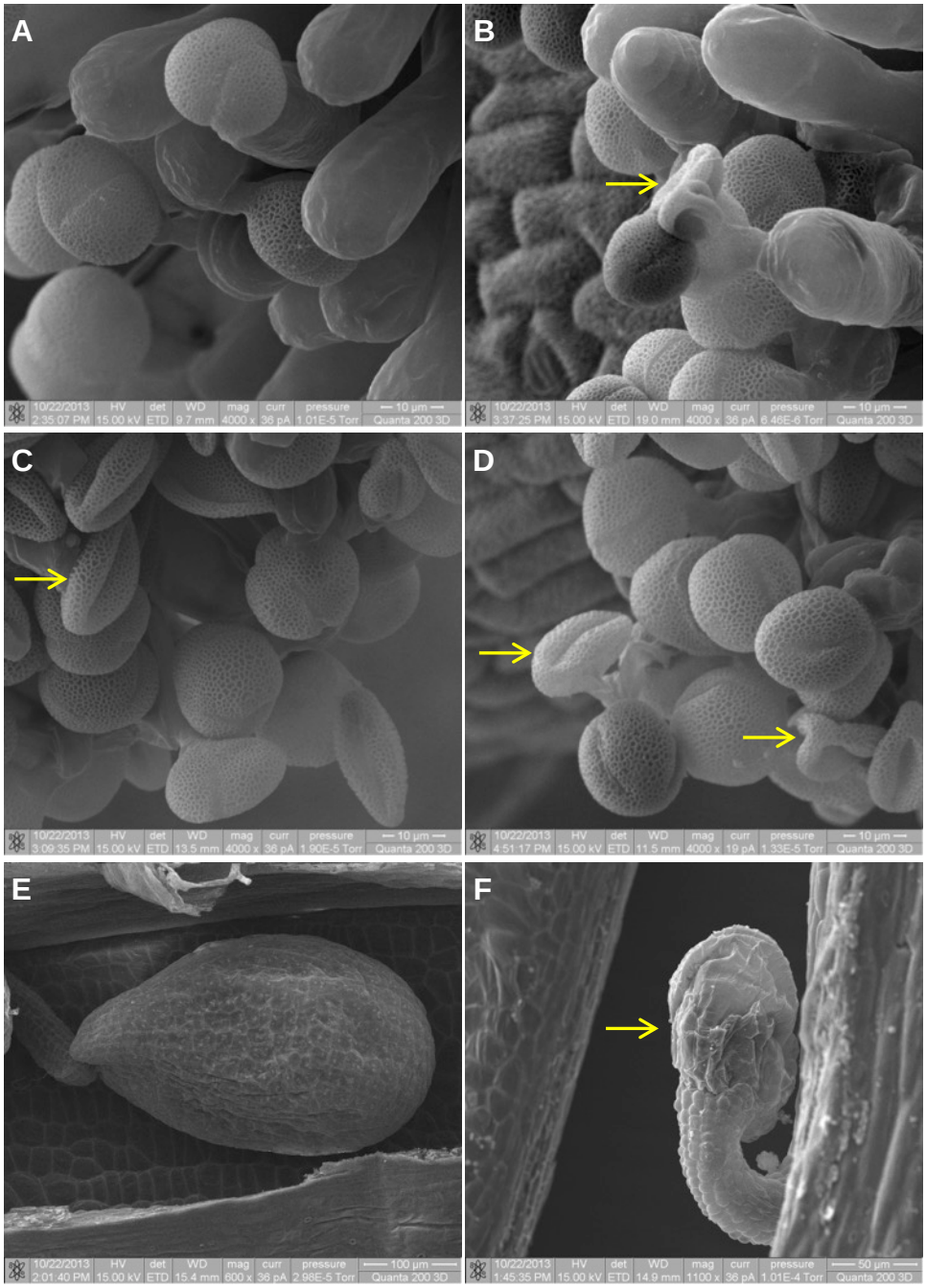

Supplemental Figure 9. SEM images of pollinated pistils and developing seeds.
(A-D) Pollinated pistils from WT (A) and double knockdown *qrt* 260-1 (B), ami356-1 (C) and ami260-4 (D) opened flowers (stages late 13 and 14). Yellow arrows indicate pollen grains with defects in pollen rehydration showing a collapsed shape. (E-F) Developing seeds in manually opened siliques of WT (E) and ami356-1 (F) plants. Yellow arrow indicates an unfertilized ovule.

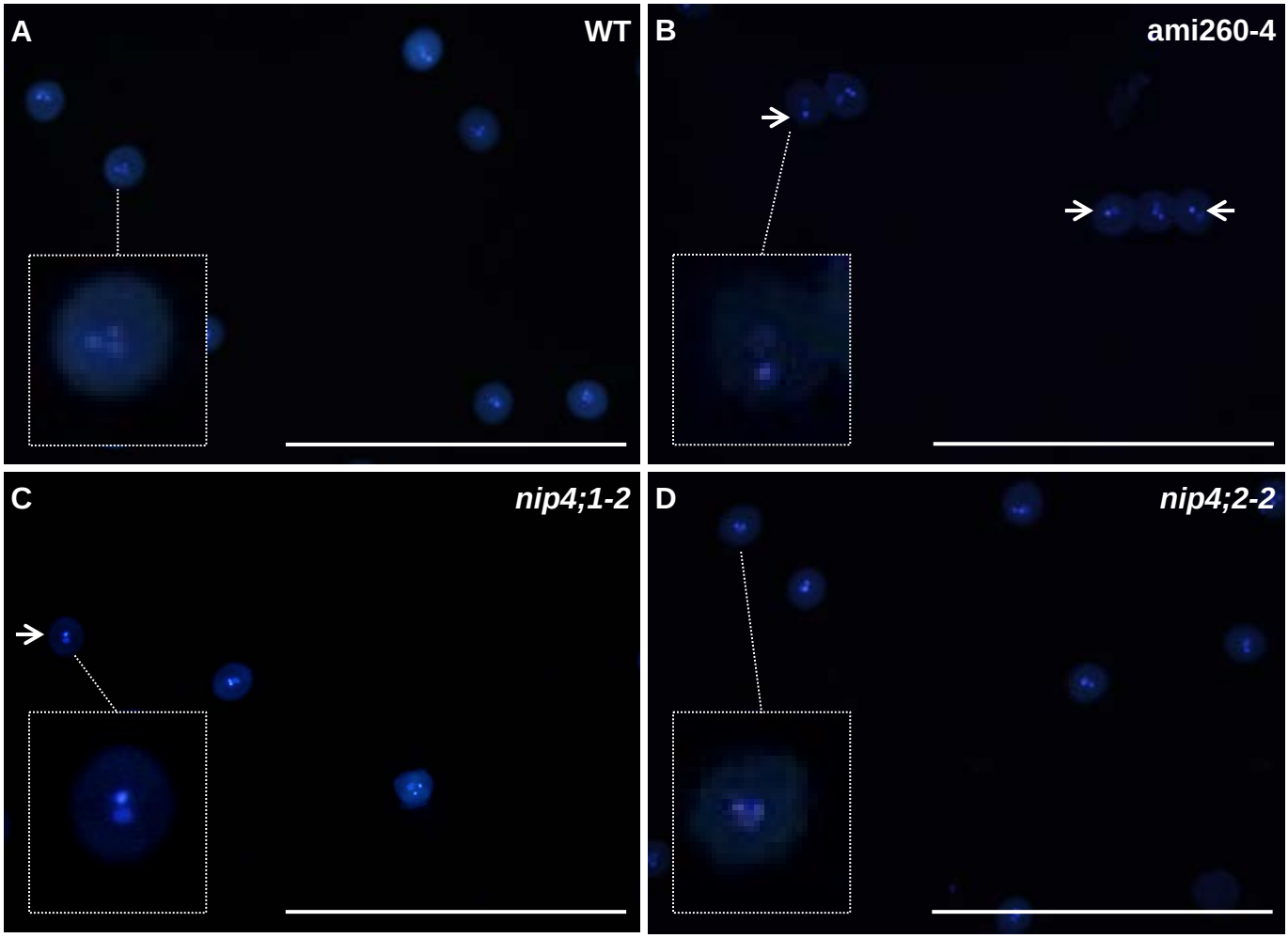

Supplemental Figure 10. Pollen microgametogenesis.
Development of WT (A), double knockdown ami260-4 (B), single mutant *nip4;1-2* (C) and *nip4;2-2* (D) pollen grains. Nuclei were stained with Hoechst 33342. Insets show a representative pollen grain in detail. White arrows indicate bicellular pollen grains. Bar = 200 µm.

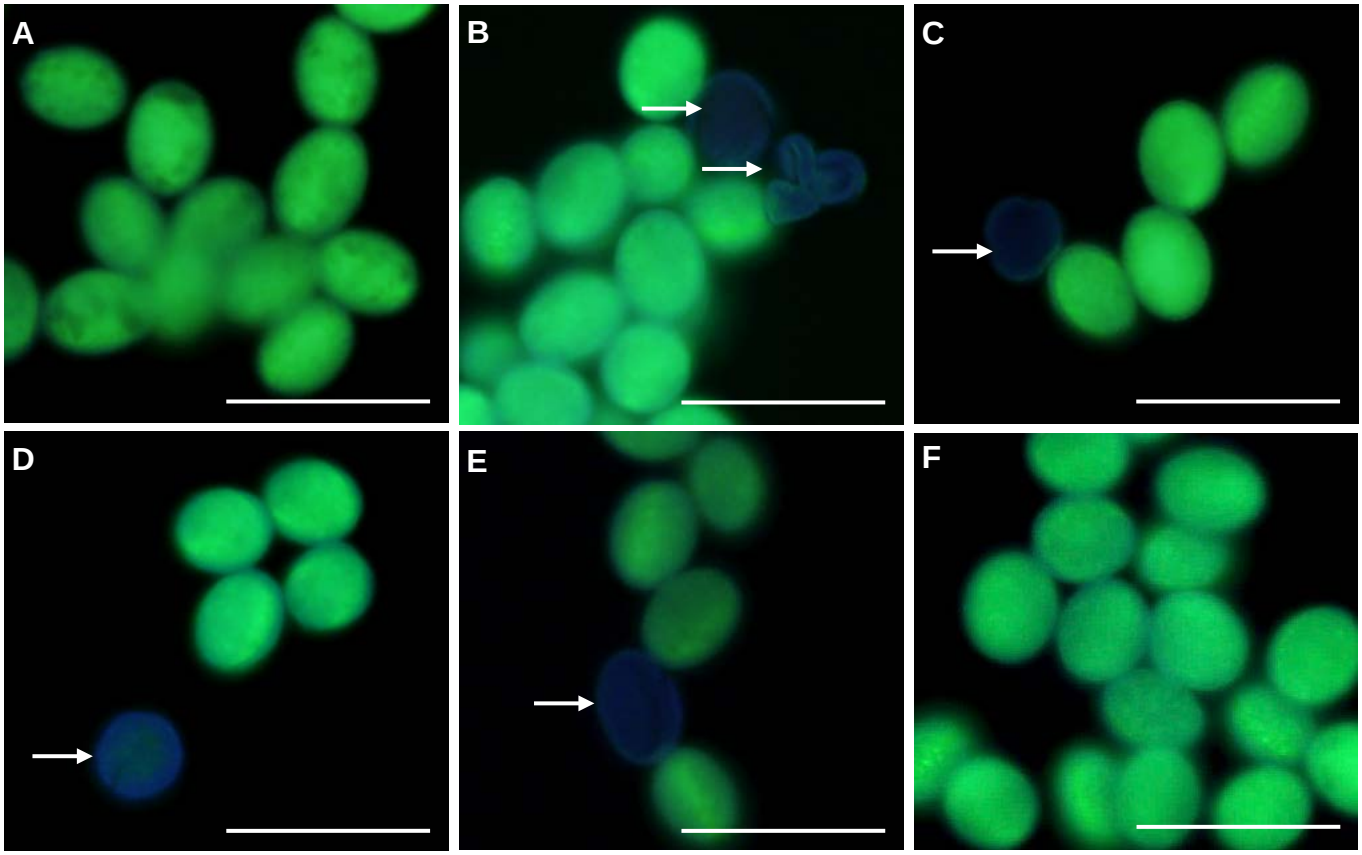

Supplemental Figure 11. Viability of mature pollen grains.
Mature pollen was stained with FDA for 10 min. Epifluorescence images of viable (green) and non-viable (blue) pollen grains of WT (A), double knockdown ami260-4 (B) and ami356-1 (C) and single T-DNA mutants *nip4;1-3* (D), *nip4;1-1* (E) and *nip4;2-1* (F). White arrows show non-viable, collapsed pollen grains. Bar = 50 µm.

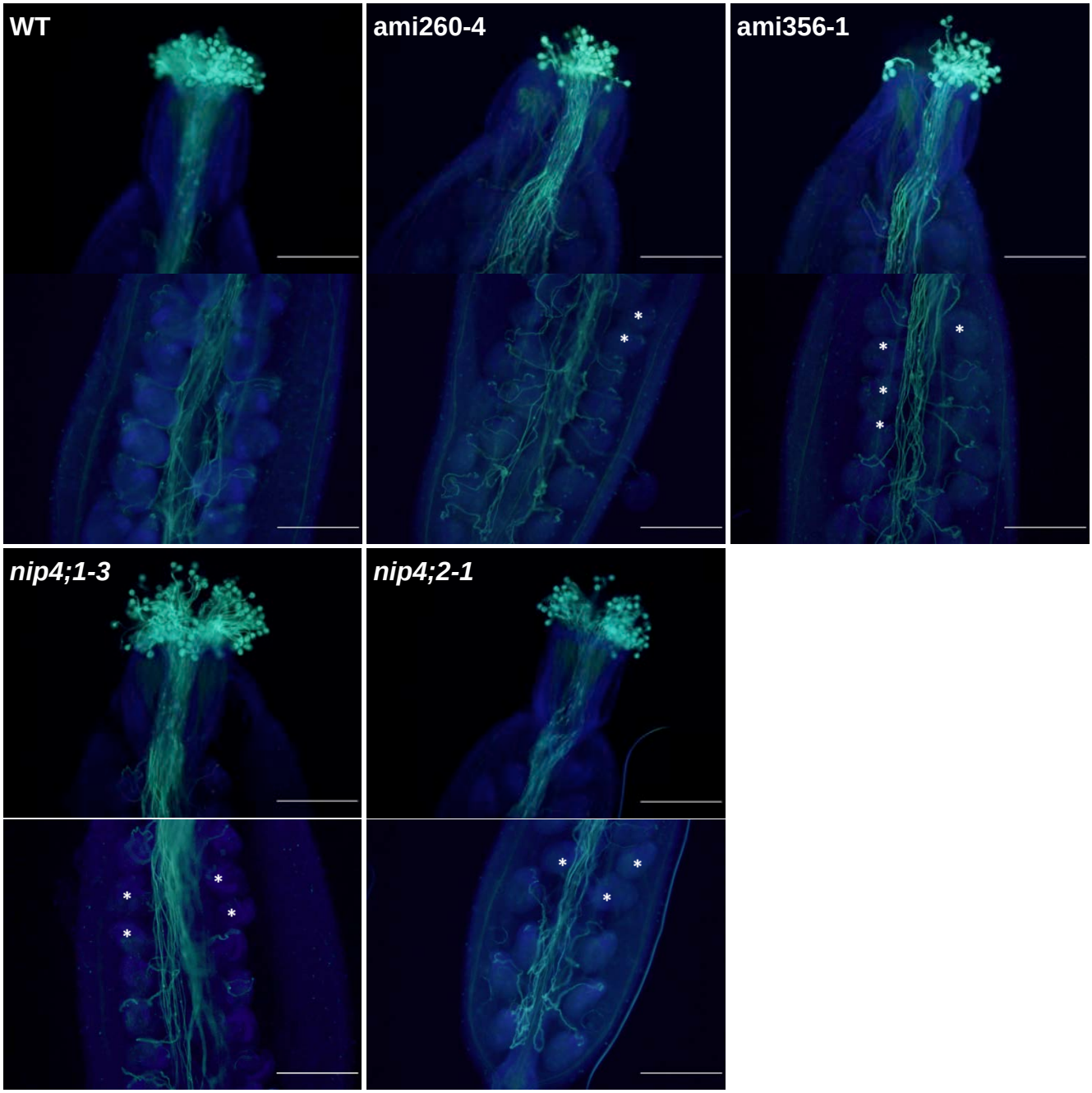

Supplemental Figure 12. Pollen tube growth in self-crossed pistils.
Decolorized aniline blue staining images of self-crossed pistils of WT (n=10), double knockdown (ami260-4, n=14 and ami356-1, n=17) and single mutant (*nip4;1-3*, n=8 and *nip4;2-1*, n=9) flowers at stage 15 post-fertilization. Only pistils with completely pollinated stigmas were analyzed. White asterisks indicate non-fertilized ovules. Bar = 200 µm.

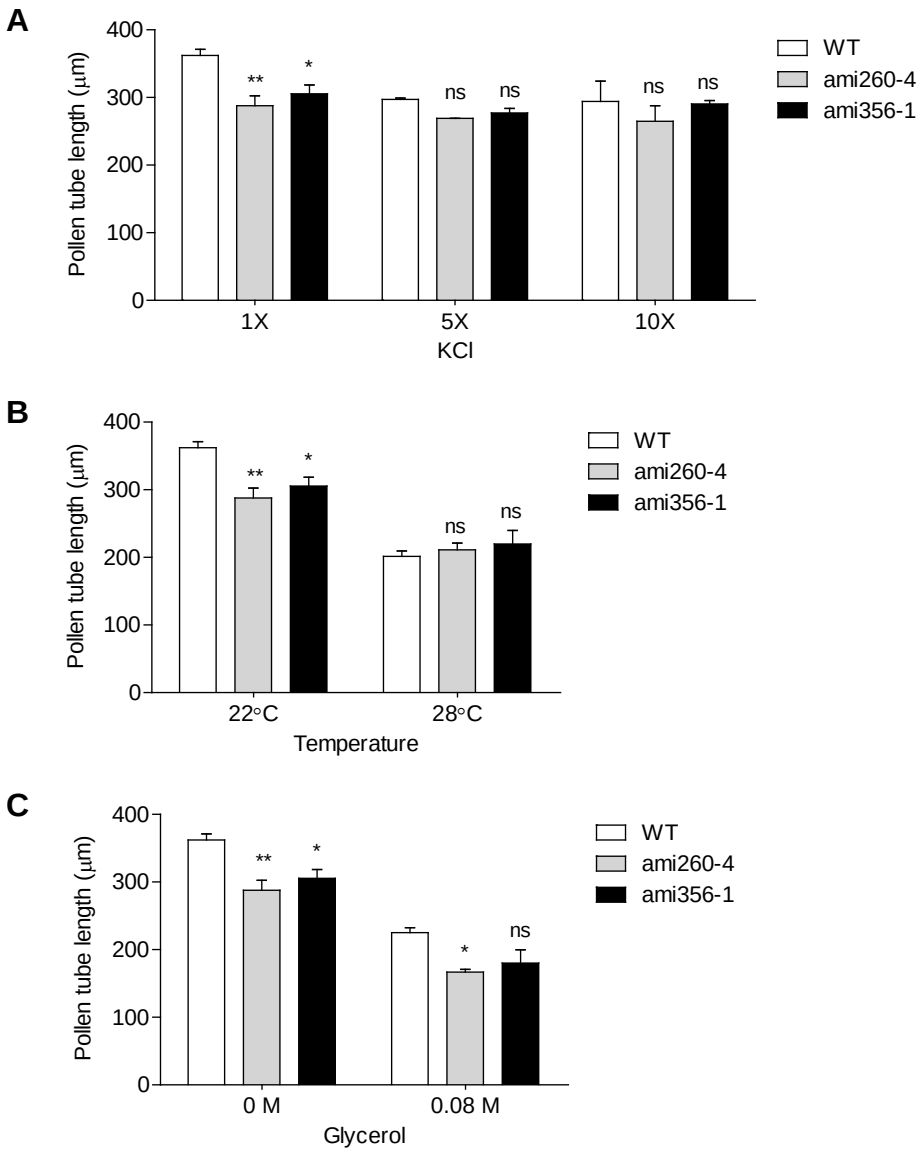

Supplemental Figure 13. Effect of temperature, salt, and osmotic stress on pollen tube growth.
(A-C) In vitro pollen germination of wild type (WT) and amiRNA (ami260-4 and ami356-1) plants on standard or modified solid PGM. Mean tube length ± SEM of ami260-4/WT and ami356-1/WT pollen germinated in solid PGM with (A) standard (1X = 5 mM KCl) or increasing salt concentrations (5X and 10X), at (B) standard (22°C) or higher (28°C) temperature, and (C) without (0 M) or with 0.08 M glycerol. Assays were performed in duplicate and repeated twice; ≥ 100 pollen tubes were measured for each replicate. Data was analyzed by one-way ANOVA and Tukey's test, (*$p<0.05$, **$p<0.01$, ns: not significant).

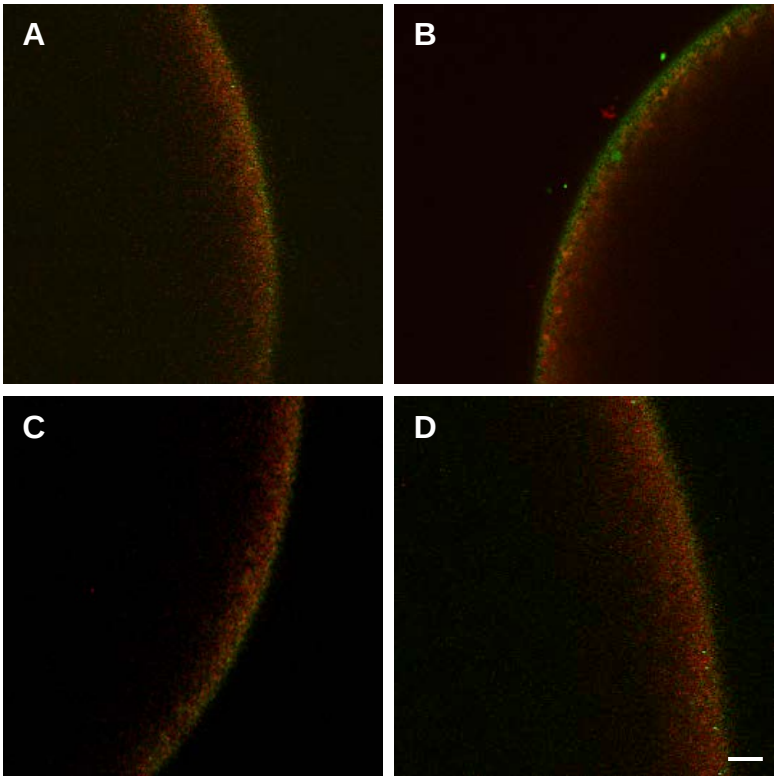

Supplemental Figure 14. Subcellular localization of EGFP-NIP4;1 and EGFP-NIP4;2 in Xenopus oocytes.
Radial (x–z) confocal images of *Xenopus laevis* oocytes expressing EGFP-NIP4;1 (A) EGFP-NIP4;2 (B), EGFP-NIP4;1-S267A (C) and EGFP-NIP4;2-S267A (D) (green), previously injected with TMR-Dextran (red). Bar = 10 µm. These are representative images of a total of three independent assays analyzing at least 20 eggs.

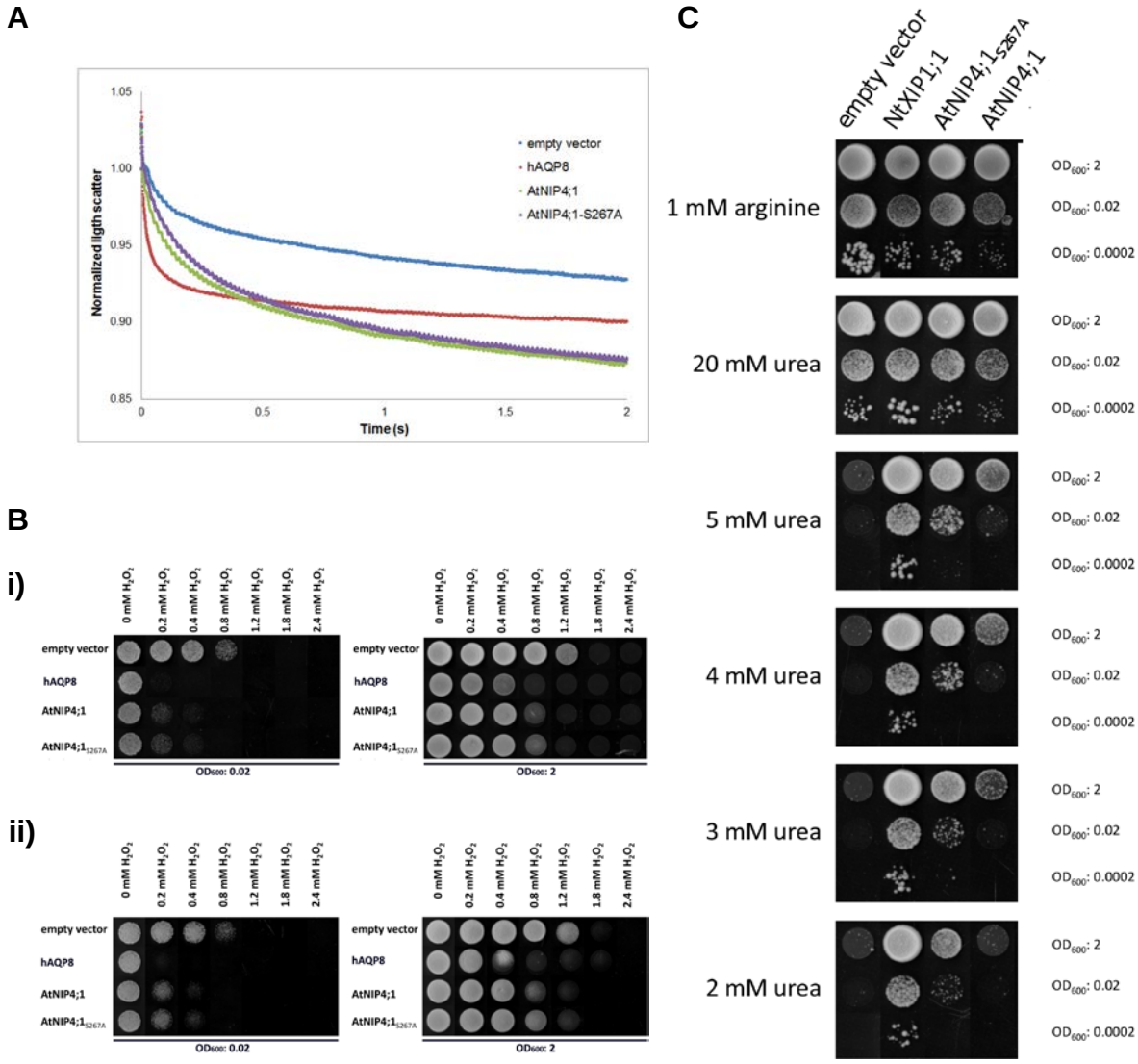

Supplemental Figure 15. Functional assays of NIP4;1 and mutant NIP4;1-S267A in yeast

(A) Water transport assays were done in yeast spheroplasts transformed with NIP4;1, NIP4;1-S267A or human AQP8 as a positive control, prepared and mixed in a stopped flow apparatus with hyposmotic solution to induce cell swelling. Spheroplasts from yeast cells (BY4741) transformed with the pYeDP60u empty vector or containing the indicated AQP homologs, were suspended in 0.5 M sorbitol plus 0.4 M potassium sulfate at an OD_{600} of 2.0 and mixed in a fast kinetics instrument with an equal volume of hypotonic buffer 0.5 M sorbitol at 10°C (300 mosmol difference). Each line represents the average of 20–30 measurements. Data points were collected each 500 µs for 3 s. Measurements from the first 2 s are displayed. Representative result of two independent experiments. (B) Yeast growth and survival on synthetic medium with different concentrations of H_2O_2. Yeast strains YNVW1 (Δdur3) (i) and Δmep1-3 (ii) transformed with the empty vector pYeDP60u or pYeDP60u containing the indicated AQP homologs, were spotted at an OD_{600} of 0.02 and 2 on medium containing various concentrations (0, 0.2, 0.4, 0.8, 1.2, 1.8, 2.4 mM) of H_2O_2. Growth was recorded after 8 days at 28°C. All data were duplicated in three independent experiments. (C) Yeast growth and survival on synthetic medium with different concentrations of urea. YNVW1 (Δdur3) yeast mutants transformed with the pYeDP60u empty vector or containing the indicated AQP homologs, were spotted at an OD_{600} of 2, 0.02 or 0.0002 on medium containing various concentrations of urea or arginine as sole nitrogen source and growth was recorded after 9 days at 28°C. All data were duplicated in three independent experiments.

SUPPLEMENTAL TABLES

Supplemental Table 1. Microgametogenesis of single mutant *nip4;1* and *nip4;2* and double knockdown pollen.

Microgametogenesis	TCP		BCP+UCP	
	Mean	SEM	Mean	SEM
WT	98.58 a	0.18	1.42 a	0.18
ami356-1	96.00 b	0.99	4.09 b	0.98
ami260-4	96.98 b	0.31	3.14 b	0.79
nip4;1-2	96.59 b	0.63	3.41 b	0.63
nip4;2-2	97.51 ab	0.30	2.49 ab	0.30

Mean percentages of tricellular (TCP), and bicellular and unicellular (BCP+UCP) ± SEM pollen grains of WT, double knockdowns ami356-1 and ami260-4 and single mutants *nip4;1-2* and *nip4;2-2*. Assays were performed in 4 replicates (i.e., plants) for each genotype. For each replicate, 10 flowers and >100 pollen grains were analyzed. Columns with different letters indicate significant difference ($p<0.05$, one-way ANOVA, Tukey's test). Collapsed-shape grains were excluded from this analysis.

Supplemental Table 2. Viability and hydration capacity of mature pollen.

FDA staining	% lethality	SEM	Relative volume	SEM
WT	2.32 a	0.32	1.00 a	0.02
ami260-4	6.24 b	1.12	0.72 b	0.04
ami356-1	6.72 b	0.76	0.75 b	0.03
nip4;1-1	5.27 b	0.48	0.81 b	0.01
nip4;1-3	5.47 b	0.68	0.73 b	0.02
nip4;2-1	3.28 ab	0.60	0.96 a	0.03
nip4;2-2	3.02 ab	0.65	0.92 a	0.02

Mean lethality percentage and relative volume ± SEM of WT, double knockdowns ami356-1 and ami260-4, and single mutants *nip4;1-1* and *nip4;1-3* and *nip4;2-1* and *nip4;2-1*. Assays were performed in 6 replicates (i.e. plants) per genotype. For each replicate 5-8 flowers incubated for 10 min with FDA and 100 and 30 pollen grains were analyzed for viability and volume assays, respectively. Different letters indicate significant difference ($p<0.05$, one-way ANOVA, Tukey's test).